Published in IET Microwaves, Antennas & Propagation
Received on 19th November 2008
Revised on 21st July 2009
doi: 10.1049/iet-map.2008.0400

ISSN 1751-8725

Microstrip-fed broadband circularly polarised monopole antenna

J.-W. Wu[1] J.-Y. Ke[1] C.F. Jou[1] C.-J. Wang[2]

[1]Department of Communication Engineering, National Chiao Tung University, Hsinchu, Taiwan
[2]Department of Electrical Engineering, National University of Tainan, Tainan, Taiwan
E-mail: cjwang@mail.nutn.edu.tw

Abstract: A microstrip-fed broadband circularly polarised (CP) monopole antenna was studied. A broad impedance bandwidth and wide axial ratio bandwidth (AR-BW) could be achieved simultaneously. This antenna used a conventional monopole architecture, except for its deforming ground plane and asymmetric-feed approach. The asymmetric-feed was used to provide an orthogonal component distinct from its original linear polarisation. In addition, by embedding a slit and a stub on the ground plane, this antenna could generate CP wave radiation and achieve a broad impedance bandwidth. According to the measurement results, the impedance bandwidth was 6.56 GHz for a 10 dB return loss, which covered a range of 2.32–8.88 GHz. The AR-BW was 1.2 GHz for a 3 dB AR, which covered a range of 3.2–4.4 GHz.

1 Introduction

Recent applications of circularly polarised (CP) waves have attracted much attention due to their significant superiority in resisting inclement weather as compared to linearly polarised (LP) waves. In particular, they have been employed in modern communication systems that are sensitive to atmospheric variations, such as radar tracking, navigation, satellite systems and mobile communication systems [1]. The hazard caused by misalignment can be ignored to simplify antenna mounting as well as to improve reception efficiency. Exciting a CP wave requires two conditions: first, the amplitudes of two near-degenerate orthogonal $\boldsymbol{E}$ vectors must be equal; second, the phase difference (PD) between the two orthogonal $\boldsymbol{E}$ vectors must be approximately 90°. Right-hand circular polarisation (RHCP) or left-hand circular polarisation (LHCP) can be defined by a 90° phase lead or lag. Traditionally, a polariser has been required for exciting a quadrature phase contribution to produce CP. To do so, some approaches have employed couplers, dividers or phase shifters to provide a 90° PD [2]. These mechanisms have been referred to as the so-called dual-feed technique. On the other hand, some researchers established a cavity model to estimate the central frequency of CP and the polarised sense based on the physical dimensions and feeding positions of the antenna [3–5]. These configurations enabled CP capability to be realised using a single-feed method, which simplified the feeding networks.

In addition to patch antennas, many types of antennas can effectively generate CP, such as slot antennas [6], helical antennas [7] and arrays [8]. In recent years, many studies have designed CP monopole antennas. In 1998, Ojiro used a monopole feed and a symmetrical loop to generate a travelling wave current and realise CP [9]. A coplanar waveguide (CPW)-fed monopole antenna with a shorting sleeve strip was used to excite a CP mode by the coupling effect between the monopole antenna and sleeve [10].

This paper proposes a microstrip-fed monopole antenna to achieve a broad impedance bandwidth and wideband CP. This antenna is composed of an asymmetric feed line, a rectangular radiator and a ground plane with an embedded slit and stub. Asymmetric feeding achieves a wide impedance bandwidth and excites an elliptically polarised (EP) wave. By modifying the shape of the ground plane, this antenna simultaneously generates a broad impedance bandwidth and wideband CP. The current work presents parametric studies of the antenna geometry, and the measured results show that this antenna excites a broad impedance bandwidth of 102.5% at a centre frequency of 5.6 GHz and a wideband CP radiation wave of 31.6% with respect to a centre frequency of 3.8 GHz.

2 Operation of circular polarisation

Feeding structures are typically classified into two categories, central feeding and asymmetric feeding, which can cause different surface current distributions on an antenna. Fig. 1*a* shows the surface current distribution for central feeding, which can be divided into vertical and horizontal currents. The distribution of the horizontal current excites two components that are 180° out of phase. Therefore the radiation in the far field in the horizontal direction is very weak. Thus, it is very difficult for a conventional monopole antenna to excite CP. Asymmetric feeding, on the other hand, generates two orthogonal currents, which include the vertical and horizontal currents, as shown in Fig. 1*b*. Their amplitudes and PD cannot reach CP conditions; hence, the asymmetric feeding method can only excite an EP wave.

In general, CP is generated by two orthogonal $\boldsymbol{E}$ vectors with equal amplitudes and a 90° PD. It is defined as

$$\boldsymbol{E} = \boldsymbol{E}_{\mathrm{Hor}} + \mathrm{e}^{\mathrm{j}\delta}\boldsymbol{E}_{\mathrm{Ver}} \tag{1}$$

where $\boldsymbol{E}$ is the instantaneous electric filed vector, $\boldsymbol{E}_{\mathrm{Hor}}$ and $\boldsymbol{E}_{\mathrm{Ver}}$, respectively, denote the electric field vectors in the horizontal and vertical planes, and δ is the PD. If the amplitudes of $\boldsymbol{E}_{\mathrm{Hor}}$ and $\boldsymbol{E}_{\mathrm{Ver}}$ are equal and $\delta = \pm 90°$, the polarised wave is RHCP or LHCP [7]. In addition, the value of the axial ratio (AR) can be used to represent the characteristic of the polarisation. The AR is defined by the RHCP or LHCP [11, 12], and it is expressed as

$$\mathrm{AR} = 20\log\left|\frac{\rho+1}{\rho-1}\right| \tag{2}$$

where

$$\rho = \left|\frac{E_{\mathrm{RHCP}}}{E_{\mathrm{LHCP}}}\right| \tag{3}$$

Generally, there are three types of polarised waves: LP, EP and CP. For a perfect CP wave, the AR value is 0 dB; for a perfect LP wave, the AR value is infinite. EP is considered to lie between LP and CP. Because a perfect CP wave with AR = 0 dB is ideal, CP is typically defined based on an AR value of less than 3 dB.

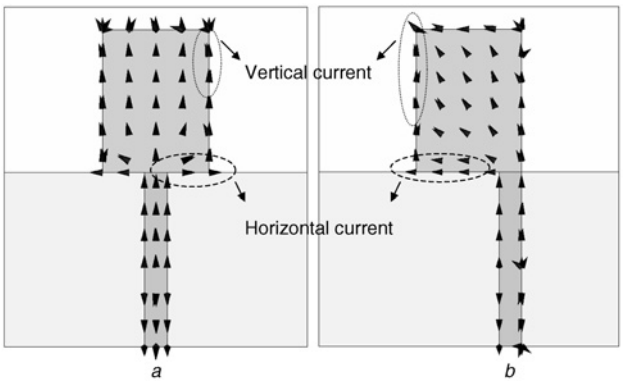

Figure 1 *Simulated surface current distributions at 3 GHz*
a Central feeding
b Asymmetrical feeding

The asymmetric feeding method generates $\boldsymbol{E}_{\mathrm{Ver}}$ and $\boldsymbol{E}_{\mathrm{Hor}}$, but it excites EP. To achieve equal amplitudes and a 90° PD, a slit was embedded on the ground plane. Using this method, the amplitudes of $\boldsymbol{E}_{\mathrm{Hor}}$ and $\boldsymbol{E}_{\mathrm{Ver}}$ were almost equal, and the phase of $\boldsymbol{E}_{\mathrm{Hor}}$ led $\boldsymbol{E}_{\mathrm{Ver}}$ with a 90° PD, which excited an LHCP radiation wave. Fig. 2 shows the simulated surface current. The amplitude difference and PD between $\boldsymbol{E}_{\mathrm{Hor}}$ and $\boldsymbol{E}_{\mathrm{Ver}}$ were varied to generate the CP mode. Furthermore, adding a stub on the ground plane further increased the impedance bandwidth, while retaining CP performance. Fig. 3 illustrates the configuration of the proposed monopole antenna. The proposed antenna was etched on an FR4 substrate with a relative permittivity $\varepsilon_{\mathrm{r}} = 4.4$, loss tangent tan $\delta = 0.024$ and thickness $H = 1.6$ mm. The top view in Fig. 3*a* shows that an asymmetric microstrip-feed line of width W_1 and length L_1 was connected to a rectangular radiator of width W_2 and length L_2. As shown in the bottom view in Fig. 3*b*, a $L_1 \times W$ ground plane was etched on the bottom side of this antenna. An $S_1 \times S_2$ rectangular slit was embedded on the ground plane, and a $D_1 \times D_2$ stub was loaded on the ground plane to the right of the slit. The overall size $(L \times W \times H)$ of the proposed antenna was approximately $45 \times 40 \times 1.6\ \mathrm{mm}^3$. Fig. 4 shows a flowchart for the design process used for the proposed CP monopole antenna.

3 Analysis of antenna design

This section describes the design techniques used for this antenna, which include increasing the impedance bandwidth and generating circular polarisation. The

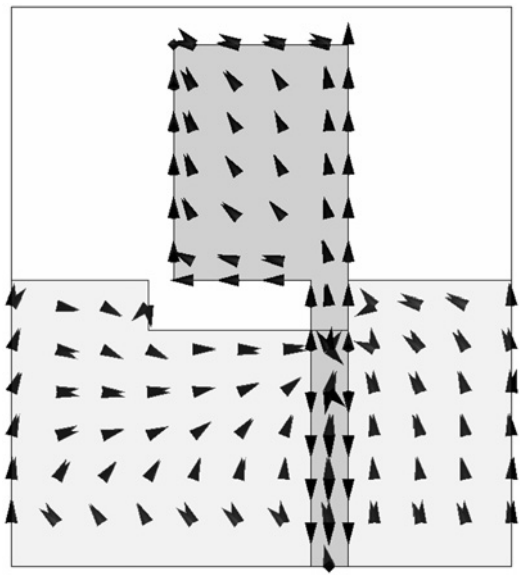

Figure 2 *Simulated surface current distributions of embedding a slit on the ground at 3 GHz*

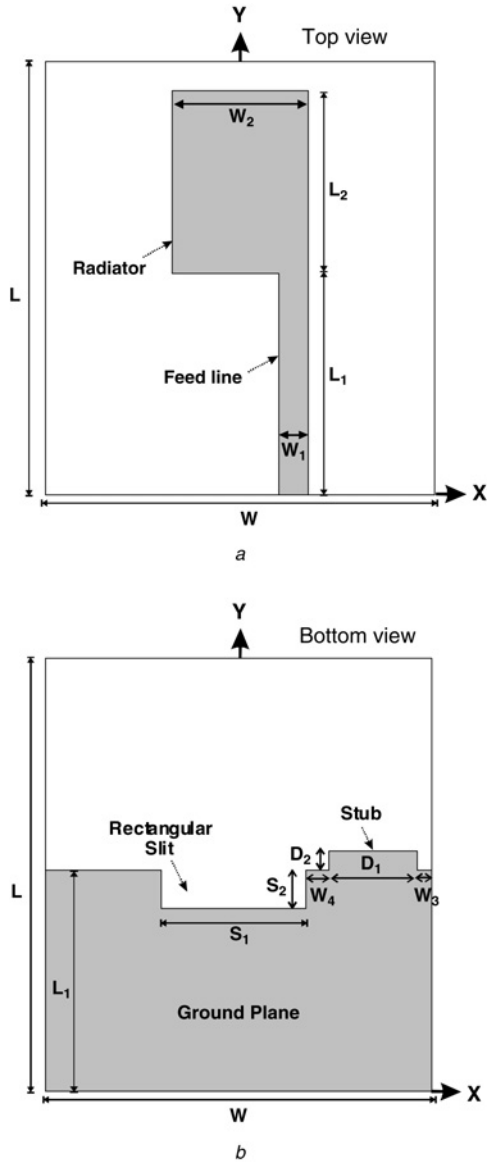

Figure 3 *Configurations of the proposed printed monopole antenna*

a Top view
b Bottom view

simulations were carried out using the finite element method software 'Ansoft High Frequency Structure Simulator' HFSS 10.0 [13].

3.1 Asymmetric feed-line

Fig. 5 describes the effects of central and asymmetric feeding on the simulated return losses. The asymmetric feeding method excited a mode at 5 GHz to increase the impedance bandwidth from 40.6% for central feeding to 82% due to via a change in the current distribution. The simulated AR results of the central and asymmetric feeding at the broadside direction are shown in Fig. 6. The centrally fed antenna radiated an LP radiation wave with an AR value greater than 40 dB. The asymmetric feeding changed the polarised wave from LP to EP, reducing the

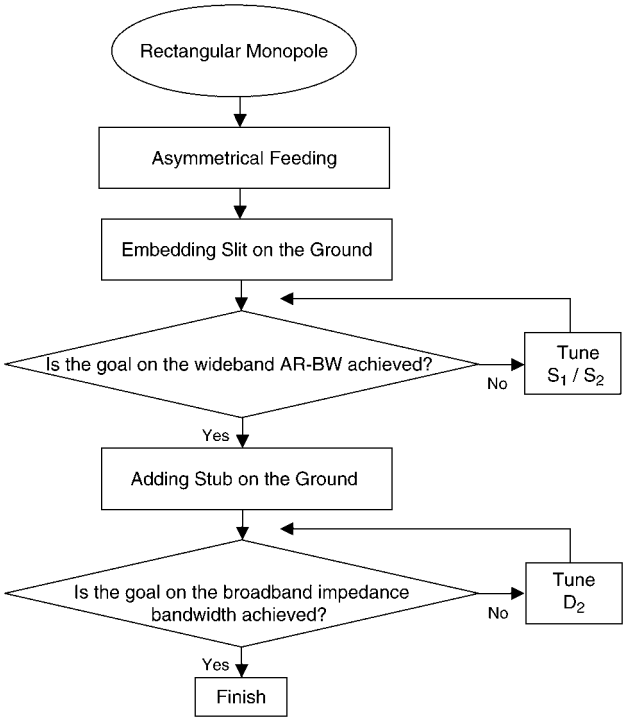

Figure 4 *Design flow chart for the proposed antenna*

AR value to approximately 7 dB at 5 GHz. Some parasitic elements were added to the ground plane to obtain a CP radiation wave. Details of the design analysis of the parasitic elements are described in the following subsections.

3.2 Embedding a slit on the ground plane

A wide impedance bandwidth and EP were generated by asymmetric feeding. To generate CP with two orthogonal currents of equal amplitude and a 90° PD, a $S_1 \times S_2$ rectangular slit was embedded on the ground plane. The performance of the impedance bandwidth and the CP were affected by the dimensions of the slit (S_1, S_2).

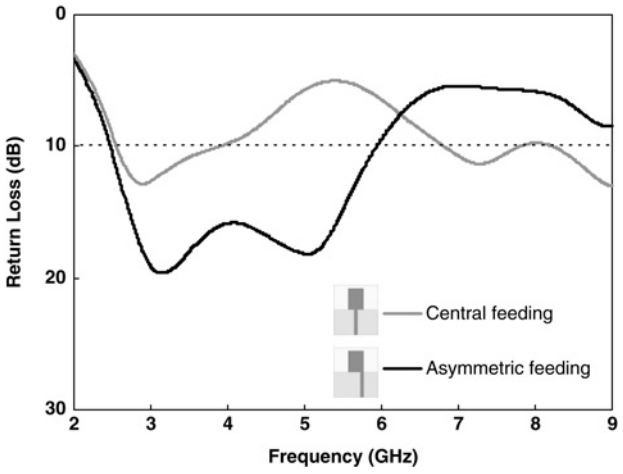

Figure 5 *Comparison the simulated return losses of central feeding and asymmetric feeding*

doi: 10.1049/iet-map.2008.0400

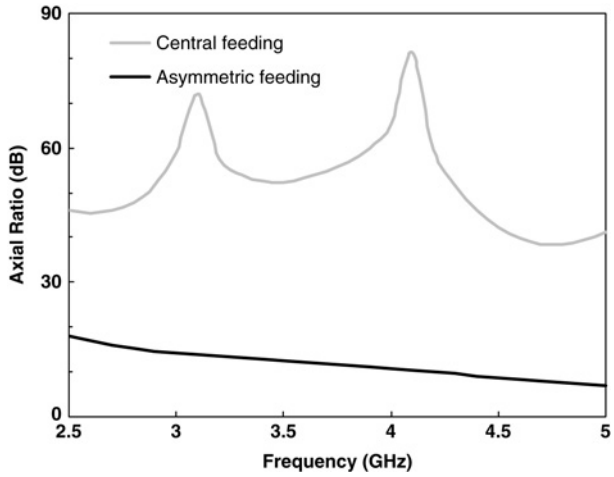

Figure 6 *Comparison the simulated AR of central feeding and asymmetric feeding*

The simulated return losses and AR of the broadside direction results with different rectangular slit lengths (S_1) are plotted in Fig. 7. With a fixed value for S_2, slits with three different lengths – 14, 15 and 16 mm – were analysed. As seen in Fig. 7*a*, the return losses from 2 to 4 GHz were affected slightly by the length S_1. However, the impedance matching was strongly dependent on S_1 from 4 to 9 GHz. In order to match the high-frequency impedance band from 4 to 9 GHz, the length of S_1 was chosen to be 16 mm. Fig. 7*b* also shows the effects of the S_1 length on the AR in the broadside direction. The findings clearly show that the CP mode frequency was not controlled by S_1, but that the widest AR-BW could be reached by properly adjusting S_1. The length of S_1 not only matched the high-frequency impedance band from 4 to 9 GHz but also tuned the AR-BW.

Figs. 8*a* and *b* depict the effects of the rectangular slit height (S_2) on the simulated return losses and AR for the

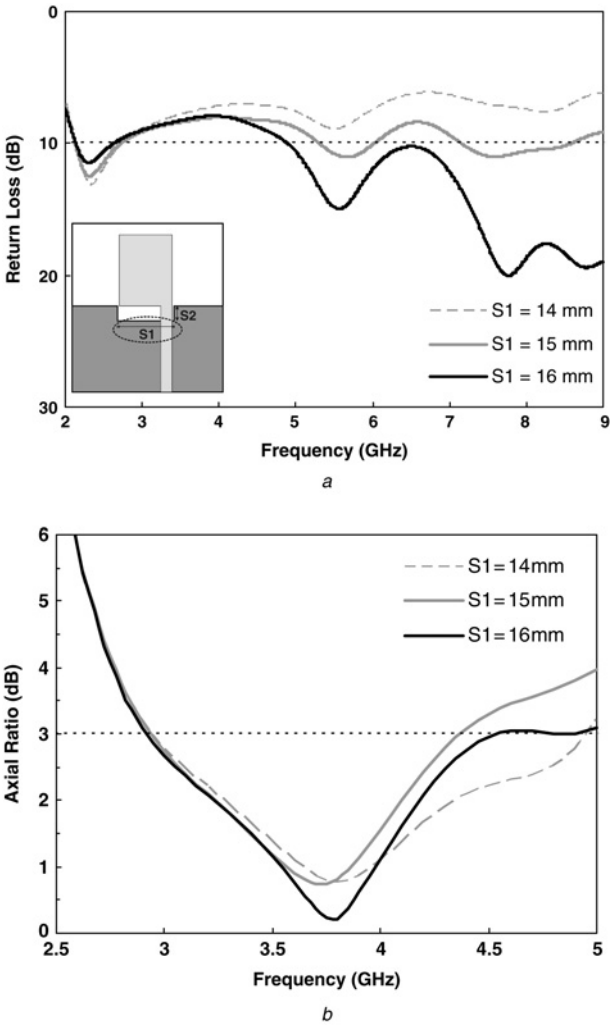

Figure 7 *Simulated return losses and AR of the rectangular slit length*

a Return losses
b AR

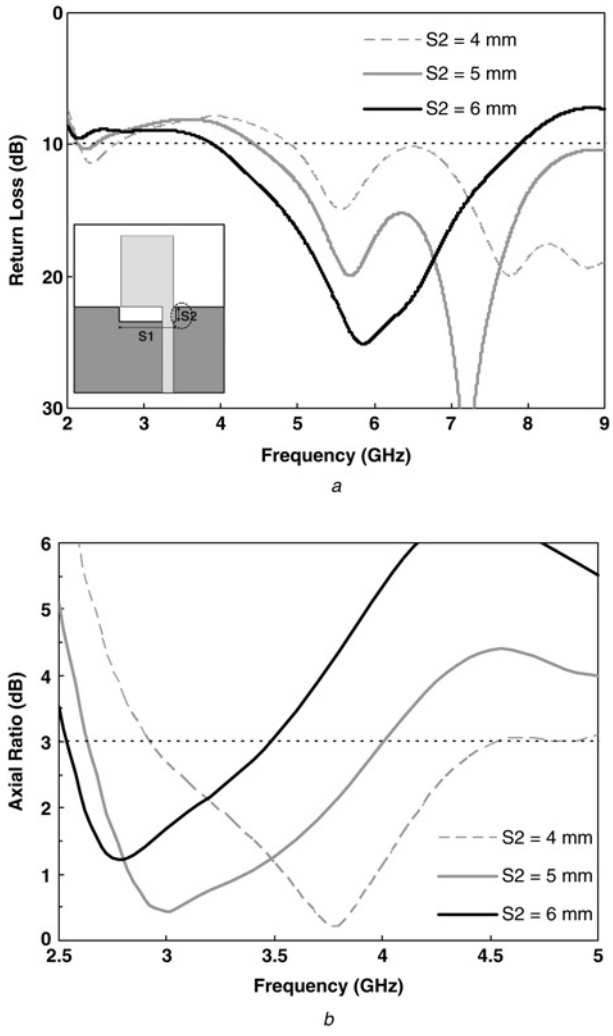

Figure 8 *Simulated return losses and AR of the rectangular slit height*

a Return losses
b AR

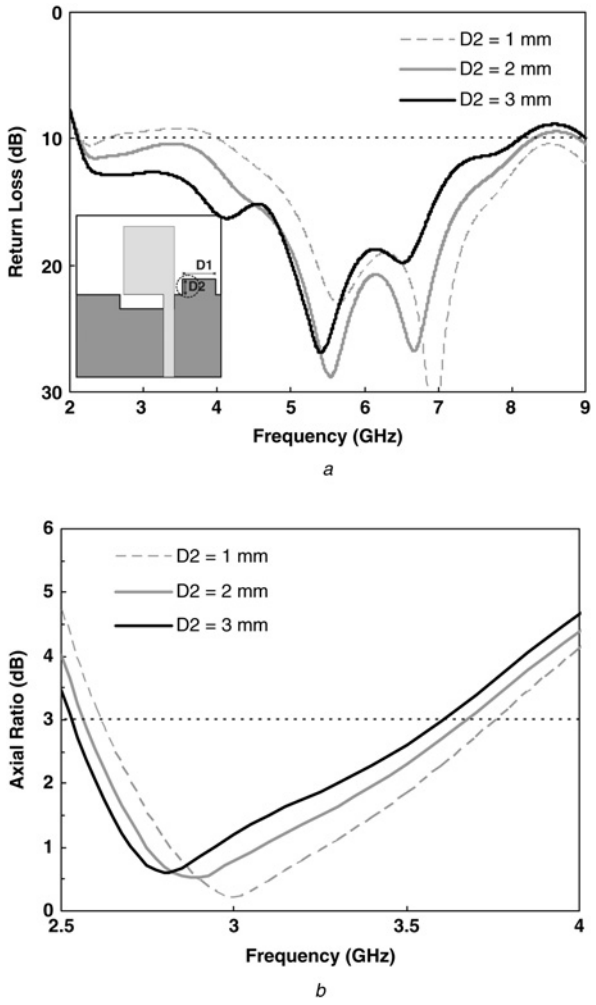

Figure 9 *Simulated return losses and AR of the stub height*
a Return losses
b AR

broadside direction results. The results in Fig. 8*a* shows that the impedance matching was strongly dependent on S_2. When S_2 was 4 mm, the third mode was at 8 GHz. When S_2 was increased to 5 mm, the third mode was shifted to 7.2 GHz. These results show that the third mode was controlled by S_2. Note that the first mode at 2.3 GHz and the second mode at 5.7 GHz were shifted only slightly.

Table 1 Dimensions of the proposed printed monopole antenna

L	45 mm	W	40 mm
L_1	23 mm	W_1	3 mm
L_2	19 mm	W_2	14 mm
S_1	16 mm	W_3	1.5 mm
S_2	4 mm	W_4	1 mm
D_1	10.5 mm	D_2	2 mm

Fig. 8*b* shows that the CP mode frequency and AR-BW could be tuned by using different values for S_2. When $S_2 = 4$ mm, the centre frequency of the CP mode was 3.75 GHz and the 3 dB AR-BW was approximately 45.3%. When S_2 was increased to 6 mm, the centre frequency of the CP mode shifted to 2.95 GHz, but the 3 dB AR-BW was only approximately 28.8%. Based on this result, the characteristics of the CP mode were also controlled by S_2.

The simulated results shown in Figs. 7*b* and 8*b* indicate that this method of embedding a rectangular slit on the ground plane excited the CP radiation wave, controlled the CP mode frequency, and achieved a wideband CP characteristic. However, a comparison of Fig. 8*a* with Fig. 5 shows that this method caused impedance mismatching from 2 to 4 GHz.

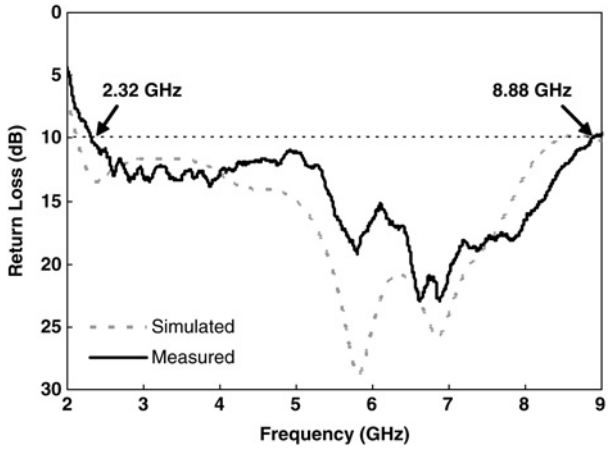

Figure 10 *Simulated and measured return losses against frequency for the proposed Antenna*

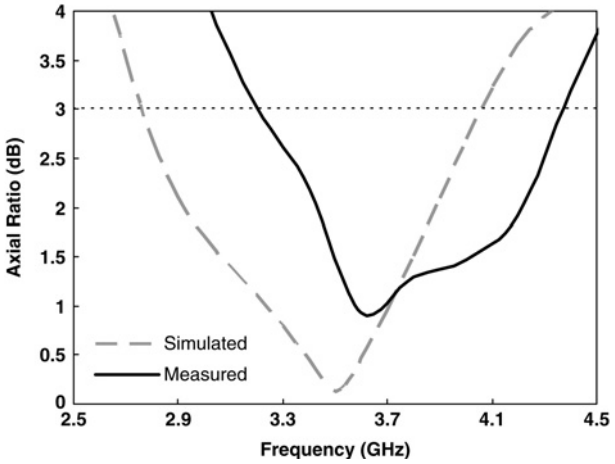

Figure 11 *Simulated and measured AR of the proposed Antenna*

doi: 10.1049/iet-map.2008.0400

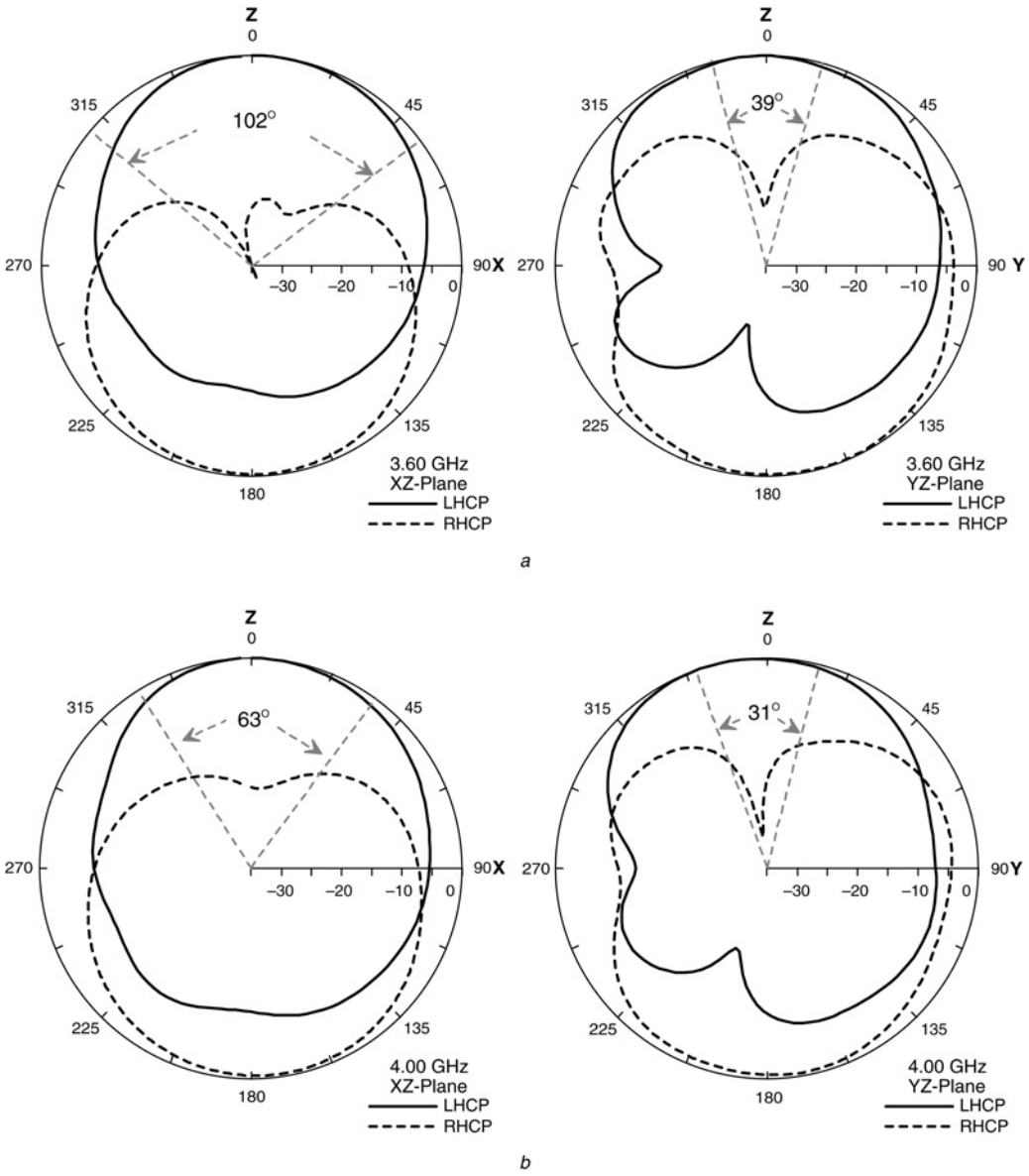

Figure 12 *Measured radiation pattern of the proposed Antenna in the XZ- and YZ-plane*

a 3.60 GHz
b 4.00 GHz

3.3 Adding a stub to the ground plane

The above discussion on the rectangular slit revealed that it generated wideband CP but caused impedance mismatching from 2 to 4 GHz, thus reducing the impedance bandwidth. To achieve a broad impedance bandwidth and still retain wideband CP, a perturbation stub was added to the ground plane on the right side of the slit. Adding the stub to the left side of the slit degraded the impedance matching.

Fig. 9 shows the simulated return losses and AR results at different stub heights (D_2), with the other parameters fixed. Fig. 9*a* shows that the mode at 4.2 GHz was excited as D_2 was increased. This phenomenon improved the impedance matching of the first mode at 2.3 GHz. In addition to impedance matching, the stub also affected the CP mode frequency. Fig. 9*b* shows that the CP mode frequency could be tuned by using different values for D_2; however, the AR bandwidth was independent of D_2. A comparison of Fig. 8*b* with Fig. 9*b* shows that the CP mode frequency was still mainly controlled by the slit height (S_2).

Based on these simulated results for asymmetric feeding with a ground plane embedded with a slit and stub, this work concludes that using asymmetric feeding enhances the impedance bandwidth and excites the EP radiation pattern. The slit embedded on the ground plane generates CP radiation waves but causes impedance mismatching in the band from 2 to 4 GHz. Adding a stub to the ground plane excites a new mode to match the impedance from 2 to 4 GHz, and only slightly affects the CP mode

characteristic. Therefore a broad impedance bandwidth and wide AR bandwidth can be simultaneously attained by properly adjusting the sizes of the slit and stub.

4 Simulation and measurement results

The optimised dimensions of the geometric parameters are listed in Table 1. A comparison of the simulated and measured return losses for the proposed antenna is shown in Fig. 10. The 10 dB impedance bandwidth of the measured return loss reached 6.56 GHz, which covers the range from 2.32 to 8.88 GHz, or approximately 117% with respect to the centre frequency of 5.6 GHz. There was good agreement between the simulated and measured results, with the exception that the measured results shifted to a higher frequency. The simulated and measured AR results for the broadside direction against frequency are plotted in Fig. 11. The disagreement between the simulated and measured results may be attributed to the phase variations of $\boldsymbol{E}_{\mathrm{Hor}}$ and $\boldsymbol{E}_{\mathrm{Ver}}$, which in turn may be due to the misalignment of the antenna and ground plane in the fabrication process. The phases of the electrical fields were very sensitive to the geometric dimensions. The measured 3 dB AR bandwidth was approximately 1.2 GHz, from 3.2 to 4.4 GHz, which corresponded to approximately 31.6% with respect to the centre frequency of 3.8 GHz. The measured minimum AR was 0.94 dB at 3.6 GHz. The measured results indicate that the proposed antenna demonstrated a broad impedance bandwidth and wide AR bandwidth.

The measured normalised LHCP and RHCP radiation patterns in the *XZ*-plane and *YZ*-plane for frequencies of 3.60 and 4.00 GHz are shown in Figs. 12*a* and *b*, respectively. Owing to the influence of the asymmetric feed line and ground plane, the CP radiation patterns of the antenna were not omnidirectional, especially in the *YZ*-plane. The measured 3 dB AR beam widths in the *XZ*- and *YZ*-planes were 102° and 39°, respectively, at 3.60 GHz, as shown in Fig. 12*a*. As seen in Fig. 12*b*, the 3 dB AR beam widths were 63° and 31° at 4.00 GHz.

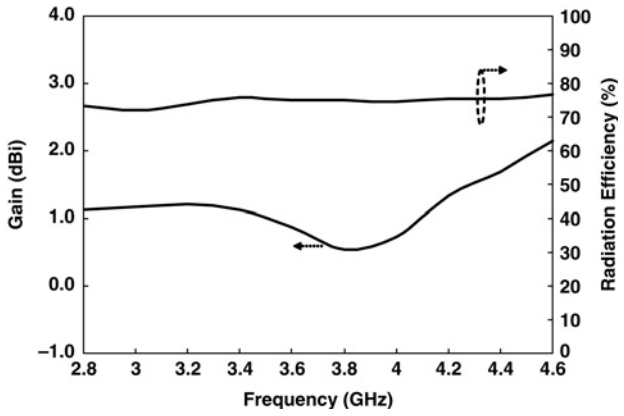

Figure 13 *Measured gain and radiation efficiency of the proposed Antenna*

Therefore the AR beam width resulted in a bigger and better performing *XZ*-plane as compared to the *YZ*-plane. Fig. 13 shows the maximum measured gains and radiation efficiencies. The efficiencies were greater than 72% from 2.8 to 4.6 GHz, and the gain variation was less than 1.6 dBi.

5 Conclusion

In this study, we developed a novel microstrip monopole antenna that is capable of realising a broad impedance bandwidth and wide AR bandwidth. It was found that asymmetric feeding changed the radiation wave from LP to EP and increased the impedance bandwidth. A rectangular slit embedded on the ground plane excited a wideband CP and controlled the frequency of the CP mode. A rectangular stub added to the ground plane enhanced the impedance bandwidth and only slightly affected the CP characteristics. The impedance bandwidth achieved measured results of 117% from 2.32 to 8.88 GHz, and a 3 dB AR bandwidth achieved results of approximately 31.6% from 3.2 to 4.4 GHz for LHCP. The proposed antenna would provide numerous advantages for a modern wireless communication system, such as low weight, simple structure, easy fabrication, low production cost, broad impedance bandwidth, and CP radiation pattern.

6 Acknowledgment

This work was supported by National Science Council, Taiwan, under grant no.: NSC 96-2221-E-024-001 and 97-2221-E009-002. The authors are grateful to thank the National Center for High-performance Computing for supports of simulation software and facilities.

7 References

[1] HSU S.H., CHANG K.: 'A novel reconfigurable microstrip antenna with switchable circular polarization', *IEEE Antennas Wirel. Propag. Lett.*, 2007, **6**, pp. 160–162

[2] WAN K.C., XUE Q.: 'A novel reconfigurable wideband circularly polarized transmitter implemented by indirect-controlled-phased-source', *IEEE Antennas Wirel. Propag. Lett.*, 2007, **6**, pp. 604–607

[3] RICHARDS W.F., LO Y.T., HARRISON D.D.: 'An improved theory for microstrip antennas and applications', *IEEE Trans. Antennas Propag.*, 1981, **29**, (1), pp. 38–46

[4] LO Y.T., ENGST B., LEE R.Q.: 'Simple design formulas for circularly polarized microstrip antennas', *IEE Proc. Microw. Antennas Propag.*, 1988, **135**, (3), pp. 213–215

[5] LEE S.K., SAMBELL A., KOROLKIEWICZ E., OOI S.F.: 'Analysis and design of a circular-polarized nearly-square-patch antenna using a cavity model', *Microw. Opt. Technol. Lett.*, 2005, **46**, (4), pp. 406–410

doi: 10.1049/iet-map.2008.0400

[6] TONG K.F., WONG T.P.: 'Circularly polarized U-slot antenna', *IEEE Trans. Antennas Propag.*, 2007, **55**, (8), pp. 2382–2385

[7] STUTZMAN W.L., THIELE G.A.: 'Antenna Theory and Design' (Wiley, New York, 1998, 2nd edn.)

[8] QIN Y., GAO S., SMABELL A.: 'Broadband high-efficiency circularly polarized active antenna and array for RF front-end application', *IEEE Trans. Microw. Theory Tech.*, 2006, **54**, (7), pp. 2910–2916

[9] OJIRO Y., HIRAGURI T., HIRASAWA K.: 'A monopole-fed circularly polarized loop antenna'. Proc. IEEE AP-S Int. Symp., June 1998, vol. 2, pp. 810–813

[10] WANG C.J., LIN Y.C.: 'New CPW-fed monopole antennas with both linear and circular polarisations', *IET Microw. Antennas Propag.*, 2008, **2**, (5), pp. 466–472

[11] IGWE G.I.: 'Axial ratio of antenna illuminated by an imperfectly circularly polarized source', *IEEE Trans. Antennas Propag.*, 1987, **AP-35**, (3), pp. 339–342

[12] TOH B.Y., CAHILL R., FUSCO V.F.: 'Understanding and measuring circular polarization', *IEEE Trans. Edu.*, 2003, **46**, (3), pp. 313–318

[13] HFSS – Ansoft Corporation: 'High Frequency Simulation Software (HFSS) Version 10.0' (Ansoft Corporation, USA)